



ELSEVIER

Contents lists available at ScienceDirect

Materials Letters

journal homepage: www.elsevier.com/locate/matlet

Synthesis and photocatalytic activity of hybrid layered ZnO(myristic acid)/Ag nanoparticles

Leslie Díaz^{a,c}, Sindy Devis^{b,e}, Clivia Sotomayor^d, Guillermo González^{b,e}, Eglantina Benavente^{a,e,*}

^a Universidad Tecnológica Metropolitana, P.O. Box 9845, Santiago, Chile

^b Universidad de Chile, P.O. Box 653, Santiago, Chile

^c Universidad de Santiago de Chile, P.O. Box 10233, Santiago, Chile

^d Catalan Institute of Nanotechnology (CIN2-CSIC) Campus Bellaterra, Spain

^e Center for the Development of Nanoscience and Nanotechnology, CEDEENNA, Santiago, Chile

ARTICLE INFO

Article history:

Received 25 January 2016

Received in revised form

4 May 2016

Accepted 28 May 2016

Available online 3 June 2016

Keywords:

Nanocomposites

Semiconductors

Photocatalysis

ABSTRACT

A new hybrid hetero nanocomposite, consisting of ZnO(myristic acid)/Ag-NPs, has been synthesized. The nanocomposite, made up of single ZnO nanosheets sandwiched between myristic acid self-assembled monolayers was synthesized and decorated with metal nanoparticles by chemical solution and tested in the photodegradation of methylene blue under UV light irradiation. The product displayed significant photocatalytic activity for degradation of the dye, and the activity was improved by a factor of three compared to bulk ZnO under similar conditions. The observed photodegradation efficiency is discussed in terms of the confinement of the semiconductor in the two dimensional structure, the adsorption ability of the organic component and the plasmonic absorption of Ag nanoparticles, which makes them act as electron wells, thus promoting charge separation and a reduced recombination rate.

© 2016 Elsevier B.V. All rights reserved.

1. Introduction

Zinc oxide (ZnO) is a semiconductor which has attracted significant attention in recent decades, due to its wide band gap of 3.37 eV, large exciton binding energy of 60 meV at room temperature and promising applications in optics and catalysis [1–4]. Low dimensional nanostructured zinc oxide structures with diverse morphologies have become particularly attractive for photocatalysis because of their catalytic efficiency, low cost and environmental friendliness [5–7]. However, their photocatalytic activity is often compromised by the rapid recombination of photoinduced electrons and holes. It has been found that, to some extent, this can be remediated by coating the surface of ZnO with noble metal nanoparticles (NPs), such as Au, Ag or Pt [8–10]. This efficiency enhancement has been ascribed to the surface plasmon resonance of Ag nanoparticles which, together with increasing photon absorption, promote interfacial charge transfer processes [11–13]. During recent years, a variety of metal-semiconductor Ag-NP/ZnO hetero nanocomposites with different morphologies have been investigated. These include ZnO NPs [14–16], thin films [17], nanofibers [18], nanorods [19,20], spheres [21], worm-like structures [22], and recently,

nanoflakes [23], nanoflowers [24] and nanowires [25] which have been successfully decorated with Ag-NPs. Ag can trap photogenerated electrons from the semiconductor, which allows holes to form hydroxyl radicals that can then react with the organic species, resulting in their degradation. In general, the degradation of dyes in the photocatalytic process is faster in the presence of a metal.

In this work, we describe the synthesis, by chemical solution methods, and the photocatalytic behavior of a new kind of ZnO-based nanostructure, namely, a hybrid layered nanocomposite, consisting of ZnO(myristic acid)/Ag-NPs. In this composite, the confinement of the semiconductor in the two dimensional structure, the adsorption ability of the organic compounds and metal nanoparticles that act as electron wells are all conjugated. The photoactivity of this nanocomposite, tested by the degradation of aqueous methylene blue by UV light irradiation, was clearly improved with respect to bulk ZnO under similar conditions.

2. Experimental

2.1. Hybrid nanocomposite, ZnO(myristic acid) and Ag nanoparticles (Ag-NPs)

Hybrid nanocomposite, ZnO(myristic acid) and Ag nanoparticles (Ag-NPs) were synthesized according to the method described previously [26,27].

* Corresponding author at: Universidad Tecnológica Metropolitana, P.O. Box 9845, Santiago, Chile.

E-mail address: ebenaven@utem.cl (E. Benavente).

Elemental analysis for $\text{ZnO}(\text{C}_{14}\text{H}_{27}\text{O}_2)_{0.2} \times 0.1\text{H}_2\text{O}$ cal. (%): C, 26.54; H, 4.160; O, 6.280. Found (%): C, 26.06; H, 4.290; O, 6.050.

2.1.1. Hybrid heteronanocomposite ZnO(myristic acid)/Ag-NPs

Nanocomposite ZnO/myristic acid (0.50 g) was mixed with the suspension of Ag NPs. The resulting suspension, after stirring for 48 h at room temperature, was aged for 48 h at room temperature. The product was separated by centrifugation, washed twice with water/acetone (1:1) mixture, and dried at 50 °C for 72 h. Thermogravimetric analysis of hybrid heteronanocomposite (Fig. S1) reveal the presence of 3.1% of Ag nanoparticles.

2.1.2. Photodegradation

The photocatalytic activity of the products was evaluated by measuring the degradation of methylene blue (MB) in water under UV illumination (mercury lamp 300 W). 20 mg of the nanocomposite and 50 mL of a $1.0 \times 10^{-5} \text{ mol L}^{-1}$ methylene blue aqueous solution were transferred to a reaction container. Prior to irradiation, the suspension was magnetically stirred in the dark for 30 min, to establish an adsorption/desorption equilibrium. Then, the suspension was irradiated with constant magnetic stirring to ensure a higher level of homogeneity of the photocatalyst in the suspension in the presence of O_2 as an electron scavenger. The MB concentration was monitored by its absorption at 665 nm from the UV–visible spectra of the solution (Perkin Elmer Lambda 35), using nanopure water as a reference.

2.1.3. Characterization

Products were characterized by thermogravimetric analysis (TG Mettler Toledo TGA/DSC 1100 SF), Powder X-ray diffraction analyses (XRD) were performed using a Siemens diffractometer D-5000 ($\text{Cu K}\alpha \lambda = 1.5418 \text{ \AA}$). Morphological studies were performed using a scanning electron microscope (SEM EVO MA 10 ZEISS) and a transmission electron microscope (TEM JEOL JEM 2200FS microscope (200 kV)). The diffuse reflectance UV–visible spectra were recorded in the range of 200–800 nm using a Perkin Elmer Lambda 35 spectrometer. Reflectance measurements were converted to absorption spectra using the Kubelka-Munk function.

3. Results and discussion

Representative XRD patterns are shown in Fig. 1. The lamellar nature is confirmed by the X-ray diffraction patterns, which display low angle reflections, characteristic of well ordered laminar arrangements. According to the positions of the $00l$ reflections in the diffraction pattern, the interlayer distances along the c -axis in this compound amounts to 39.4 Å, the other three peaks at 2θ of 31.6, 34.3 and 36.1° are attributed to the zinc oxide and the low intensity peaks at 20°–23° may be ascribed to a small excess of free myristic acid. The two additional peaks observed correspond to the reflections arising from the [111] and [200] crystallographic planes of fcc Ag (JCPDS 04-0783).

The structure of the ZnO nanocomposite remains unaltered by the presence of the Ag nanoparticles, the long chains are oriented roughly perpendicular to the layers, in agreement with the previously-proposed model for the disposition of the guest in the interlaminar space of these nanocomposites [26].

The morphology of the studied nanocomposites is illustrated in the micrographs in Fig. 2. The TEM image shows the layered nature of the composite, with multi-layer laminas. The images show that the product, ZnO(myristic acid)/Ag-NPs, consists predominately of sheets of the pristine nanocomposite with Ag NPs of about 10–25 nm in size attached to their edges (Fig. S2). Fig. 2B shows of the scheme of the photocatalytic reaction of the ZnO (myristic acid)/Ag NPs heterostructure.

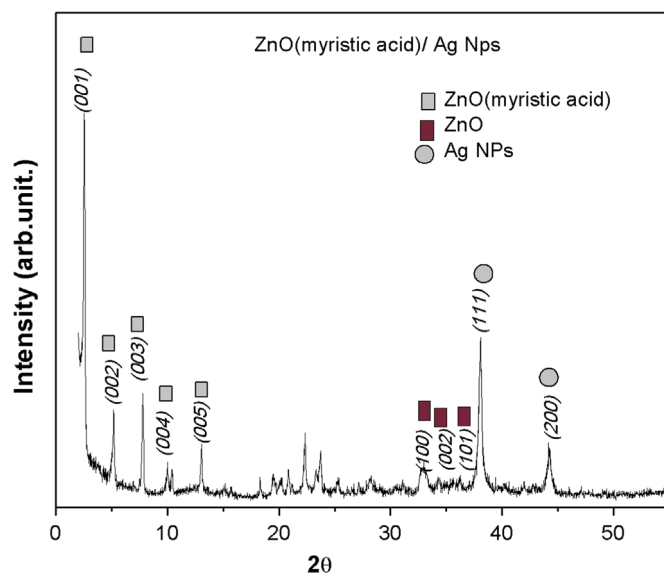


Fig. 1. X-ray diffraction patterns of hybrid layered ZnO(myristic acid)/Ag NPs.

The UV–visible diffuse reflectance was measured for ZnO, ZnO (myristic acid) and ZnO(myristic acid)/Ag-NPs to determine their light absorption characteristics, as shown in Fig. 3A. The wavelength distribution of the absorbed light is an important property of photocatalysts, irrespective of the quantum yield. Therefore, the high photoactivity was attributed to higher visible light absorbance, as indicated by UV–visible diffuse reflectance spectroscopy. The absorption bands in the range of 200–400 nm, observed in all spectra, suggest strong free exciton absorption at room temperature. The absorption band centered at 430 nm in the spectrum of the composite corresponds to the typical surface plasmon absorption, similar to that of precursor Ag NPs in the range 410–440 nm (Fig. S3), which further confirms that Ag had been deposited successfully at the surface of the nanocomposite [10,28]. In the insert of Fig. 3A, the band gap energies, E_g , determined from the spectra are 3.21, 3.37 and 3.41 eV for ZnO, ZnO(myristic acid) and ZnO(myristic acid)/Ag-NPs, respectively, the increment of the band gap of the nanocomposite, with respect to that of bulk ZnO, is clearly seen. We attribute the blue shift of the absorption band edge due to quantum confinement of the semiconductor in these lamellar structures, the separation of the energy levels of the conduction and valence bands, which increases with decreasing particle size. Such phenomenon is also detected in the absorption spectra of nanostructured ZnO species, nanoparticles and quantum dots [29,30].

In order to find out the effect of Ag NP incorporation on the photocatalytic activity of the layered ZnO(myristic acid) nanocomposites, the degradation of methylene blue by UV radiation at room temperature was selected as a model reaction. We started from a suspension of the photocatalyst, where C was the concentration of dye remaining in the solution after irradiation time t , and C_0 was the initial concentration at $t=0$. Since no degradation was observed among the products after 30 min in the dark for adsorption equilibrium, the photocatalytic behavior of the ZnO-based layered composites was compared with that of bulk ZnO. As observed in Fig. 3B, at short irradiation times, the degradation processes illustrated can be described as having pseudo-first-order kinetics, $\ln(C_0/C) = kt$, where k is the corresponding kinetic constant and t is the irradiation time. The initial reaction rate constants calculated for the three photocatalysts are compared here. As observed in Fig. 3B, ~60% degradation efficiency of the dye can be achieved at 40 min using ZnO(myristic acid)/Ag-NPs, while it accounts for about 40% and 20%, when using the nanocomposite

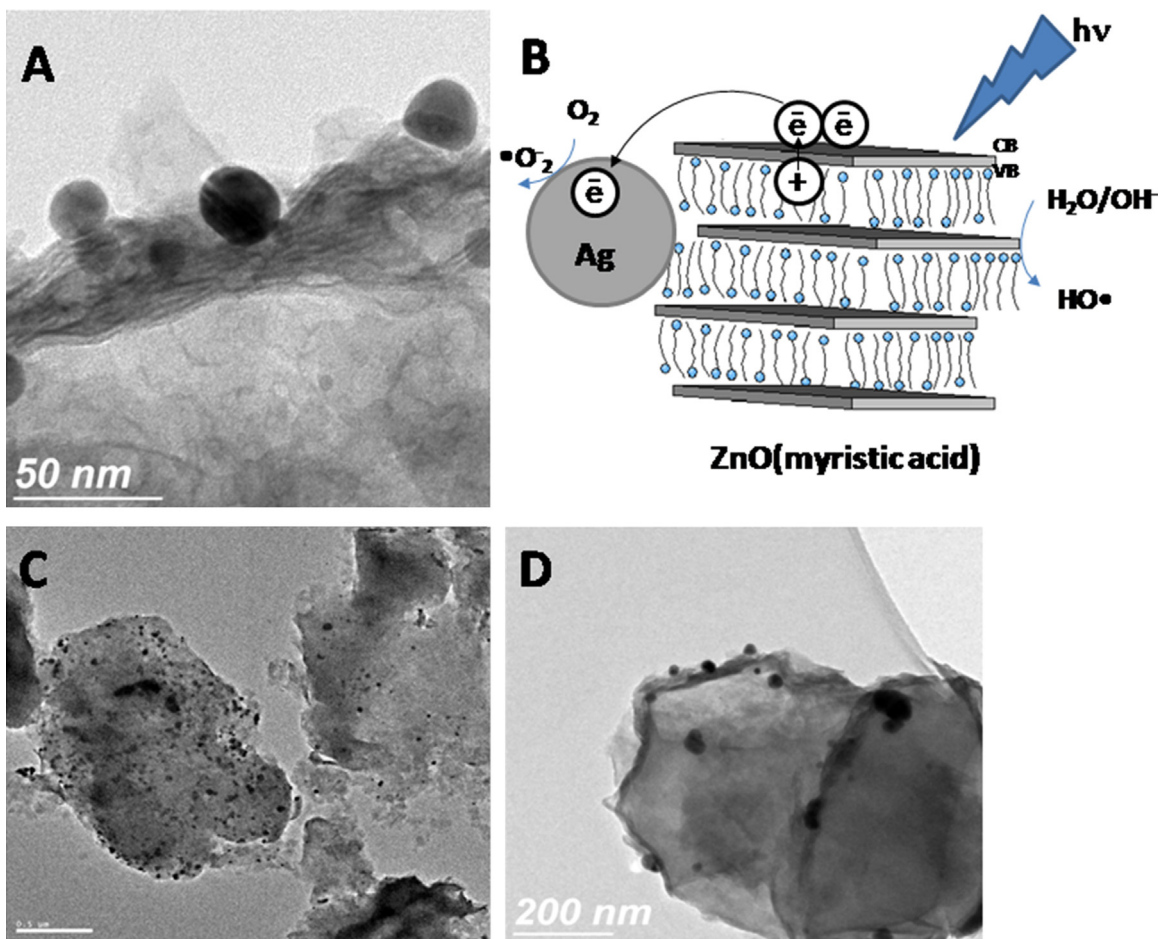


Fig. 2. A, C, D. TEM images of nanocomposites with Ag NPs. 2B. Scheme of the photocatalytic reaction of the ZnO(myristic acid)/Ag NP heterostructure.

without Ag and bulk ZnO, respectively. The photocatalytic behavior of ZnO, ZnO/(myristic acid) and ZnO(myristic acid)/Ag NPs composites under visible light irradiation also were examined (Fig. S4). As observed, the photodegradation of MB for ZnO and ZnO(myristic acid)/Ag were 17%, 25% and 30% respectively. The efficiency resulted lower than in UV light for all the samples. These results qualitatively do agree with reports on the poor harvesting of visible light of ZnO composites [31]. In Fig. 3C, the initial rate constants show the same tendency, with the reaction being about three times faster for the product containing Ag than for bulk ZnO. It is known that photocatalytic redox reactions mainly take place on the surface of the photocatalysts, and therefore, surface properties, such as area and the adsorption ability of the organic component [32], also have to be considered to understand the efficiency of photocatalysts. The XRD pattern of ZnO(myristic acid)/Ag Nps after photocatalysis cycle (Fig. S5) indicated that the composite retained its lamellar nature but lost some crystallinity.

A probable mechanism for the degradation of MB over ZnO(myristic acid)/Ag-NPs is schematically illustrated in Fig. 2B. During irradiation, in the semiconductor an electron (e^-) in the valence band can be excited to the conduction band. Meanwhile, a hole (h^+) in the valence band is generated. The photoelectron can be easily transferred to the Ag NPs and then trapped by electronic acceptors (adsorbed O_2). They are further transformed to a superoxide radicals ($\bullet O_2^-$). Further reduction of $\bullet O_2^-$ would generate peroxide intermediates which decompose to hydroxyl radicals capable of accomplishing the dye mineralization. At the same time, the photoinduced holes can be trapped by surface hydroxyl and produce hydroxyl radicals ($\cdot OH$) [15,19,31]. However, the

hydrophilic/hydrophobic balance on the surface of the photocatalyst is also important, particularly in the degradation of organic species. This may explain, at least in part, the better efficiency of the nanocomposites with respect to the native oxide, which is much more hydrophilic. The absorption of MB in dark into the nanocomposite ZnO(myristic acid) is about three times higher than into the ZnO (Fig. S6). Thus the organic layer, facilitating the dye absorption would improve its interaction with the dye.

Considering the similarity of the structural and optical properties of the nanocomposites discussed above, the improved photocatalytic activity of the product containing Ag NPs, which favored the effective electron-hole separation, preventing photo-induced electrons from migrating to the interface, inhibiting recombination [18,27]. In such a context, the surface plasmon resonance of Ag NPs has to be considered. It is expected that the presence of Ag-NPs enhances the absorption of incident photons, thus promoting interfacial charge transfer, allowing the holes to form hydroxyl radicals, able to react with the pollutants adsorbed onto the surface of the photocatalyst, thus enhancing its activity.

4. Conclusions

In summary, we describe the synthesis and properties of a new hybrid hetero nanocomposite, consisting of ZnO(myristic acid)/Ag-NPs, obtained from the reaction of layered ZnO hybrids with Ag metal nanoparticles, which significantly improved the photocatalytic behavior of the material. The photocatalytic activity of the

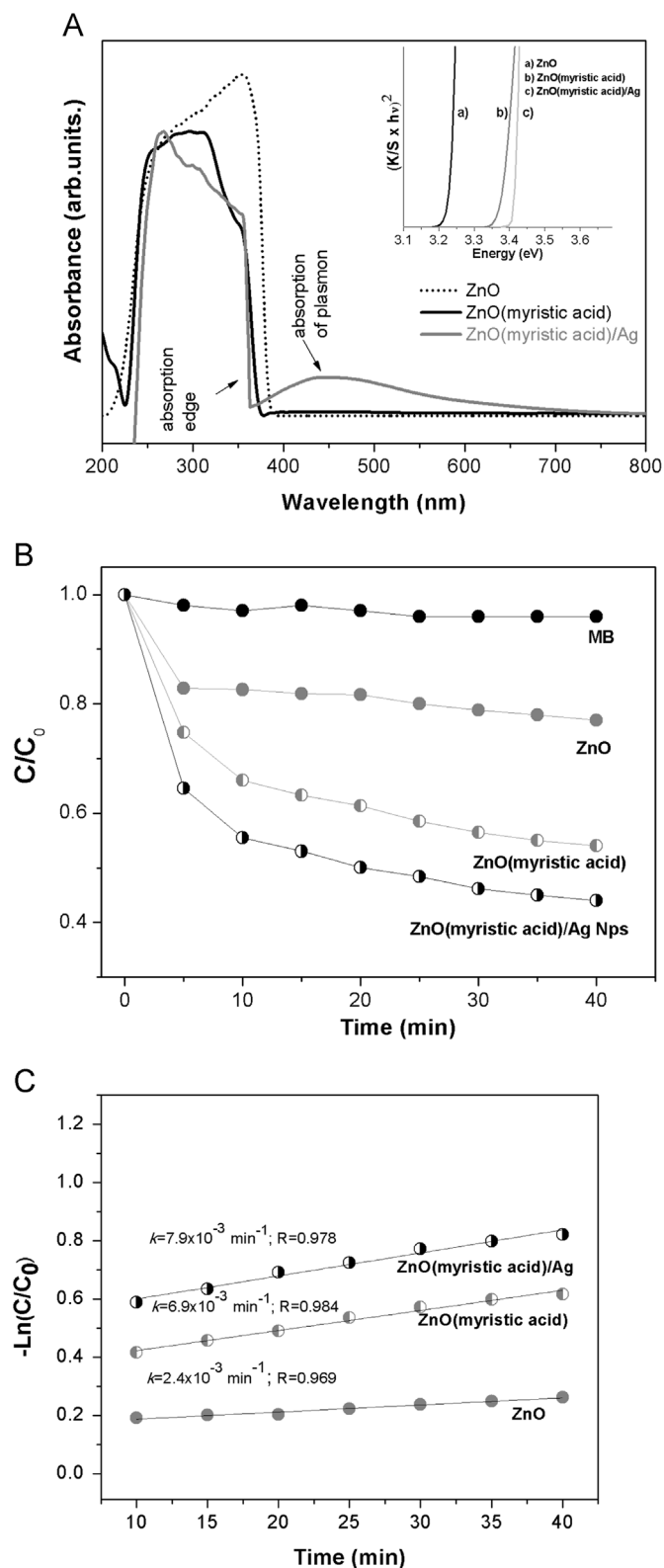


Fig. 3. **A.** UV – visible diffuse absorption spectra of the ZnO, ZnO(myristic acid) and ZnO(myristic acid)/Ag NPs. The insert shows the band gaps. **B.** Plots of the degradation of MB solution without catalyst, ZnO, ZnO(carboxylic acid) and ZnO(myristic acid)/Ag NPs under UV irradiation. **C.** Kinetics of ZnO, ZnO(carboxylic acid) and ZnO(myristic acid)/Ag NPs.

ZnO(myristic acid)/Ag-NP composite was found to be three times better than that of its precursor. We suggest that this is due to a combination of effects, namely the confinement of the semiconductor in the two dimensional structure, the adsorption ability of the organic component and the plasmonic absorption of Ag-NPs. The hybrid layered nanocomposite is a very good candidate for UV light photocatalysis compared to bulk ZnO.

Acknowledgements

The authors acknowledge the Universidad Tecnológica Metropolitana, Universidad de Chile, FONDECYT Grants 1151189 and 1131112 and CONICYT Grant FB0807 (CEDENNA) and a PhD fellowship.

Appendix A. Supplementary material

Supplementary data associated with this article can be found in the online version at <http://dx.doi.org/10.1016/j.matlet.2016.05.126>.

References

- [1] H. Tong, S.X. Ouyang, Y.P. Bi, N. Umezawa, M. Oshikiri, J.H. Ye, *Adv. Mater.* 24 (2012) 229–251.
- [2] A. Kudo, Y. Miseki, *Chem. Soc. Rev.* 38 (2009) 253–278.
- [3] D. Costenaro, F. Carniato, G. Gatti, L. Marchese, C. Bisio, *New J. Chem.* 38 (2014) 6205–6211.
- [4] J. Das, D. Khushalani, *J. Phys. Chem. C* 114 (2010) 2544–2550.
- [5] X. Wang, W. Cai, Y. Lin, G. Wang, C. Liang, *J. Mater. Chem.* 20 (2010) 8582–8590.
- [6] N. Huang, J. Shu, Z. Wang, M. Chen, C. Ren, W. Zhang, *J. Alloy. Compd.* 648 (2015) 919–929.
- [7] C.F. Tan, W.L. Ong, G.W. Ho, *ACS Nano* 9 (2015) 7661–7670.
- [8] V. Subramanian, E.E. Wolf, P.V. Kamat, *J. Phys. Chem. B* 107 (2003) 7479–7485.
- [9] C. Mondal, J. Pal, M. Ganguly, A. Kumar, J. Jana, T. Pal, *New J. Chem.* 38 (2014) 2999–3005.
- [10] P. Fageria, S. Gangopadhyay, S. Pande, *RSC Adv.* 4 (2014) 24962–24972.
- [11] W.L. Ong, S. Natarajan, B. Kloostera, G.W. Ho, *Nanoscale* 5 (2013) 5568–5575.
- [12] A. Wood, M. Giersig, P. Mulvaney, *J. Phys. Chem. B* 105 (2001) 8810–8815.
- [13] P.V. Kamat, *J. Phys. Chem. B* 106 (2001) 7729–7744.
- [14] J. Rashid, M.A. Barakat, N. Salah, S.S. Habib, *RSC Adv.* 4 (2014) 56892–56899.
- [15] R. Georgekutty, M.K. Seery, S.C. Pillai, *J. Phys. Chem. C* 112 (2008) 13563–13570.
- [16] M. Khademalrasool, M. Farbod, A. Iraj, *J. Alloy. Compd.* 664 (2016) 707–714.
- [17] A. Rajan, H. Kumar, V. Gupta, M. Tomar, *J. Mater. Sci.* 48 (2013) 7994–8002.
- [18] D. Lin, H. Wu, R. Zhang, W. Pan, *Chem. Mater.* 21 (2009) 3479–3484.
- [19] Z. Wu, C. Xu, Y. Wu, H. Yu, Y. Tao, H. Wan, F. Gao, *Cryst. Eng. Commun.* 15 (2013) 5994–6002.
- [20] K. Saoud, R. Alsoubaihi, N. Bensalah, T. Bora, M. Bertino, J. Dutta, *Mater. Res. Bull.* 63 (2015) 134–140.
- [21] J. Xie, Q. Wu, *Mater. Lett.* 64 (2010) 389–392.
- [22] H.R. Liu, G.X. Shao, J.F. Zhao, Z.X. Zhang, Y. Zhang, J. Liang, X.G. Liu, H.S. Jia, B. S. Xu, *J. Phys. Chem. C* 116 (2012) 16182–16190.
- [23] Y.V. Kaneti, J. Yue, X. Jiang, A. Yu, *J. Phys. Chem. C* 117 (2013) 13153–13162.
- [24] S.A. Ansari, M.M. Khan, M.O. Ansari, J. Lee, M.H. Cho, *J. Phys. Chem. C* 117 (2013) 27023–27030.
- [25] W.L. Ong, K.W. Yew, C.F. Tan, T.K. Tan Adrian, M. Honga, G.W. Ho, *RSC Adv.* 4 (2014) 27481–27487.
- [26] M. Segovia, K. Lemus, M. Moreno, M.A. Santa Ana, G. González, B. Ballesteros, C. Sotomayor, E. Benavente, *Mater. Res. Bull.* 46 (2011) 2191–2195.
- [27] W. Lu, S. Gao, J. Wang, *J. Phys. Chem. C* 112 (2008) 16792–16800.
- [28] Y.H. Zheng, L.R. Zheng, Y.Y. Zhan, X.Y. Lin, Q. Zheng, K.M. Wei, *Inorg. Chem.* 46 (2007) 6980–6986.
- [29] K.F. Lin, H.M. Cheng, H.C. Hsu, L.J. Lin, W.F. Hsieh, *Chem. Phys. Lett.* 409 (2005) 208–211.
- [30] J.G. Lu, Z.Z. Ye, Y.Z. Zhang, Q.L. Liang, Z.L. Wang, *Appl. Phys. Lett.* 89 (2006) 023122.
- [31] Y. Liang, N. Guo, L. Li, R. Li, G. Ji, S. Gan, *New J. Chem.* 40 (2016) 1587–1594.
- [32] J. Zhao, T. Wu, K. Wu, K. Oikawa, H. Hidaka, N. Serpone, *Environ. Sci. Technol.* 32 (1998) 2394–2400.